Improvement by solid dispersion of the bioavailability of KRN633, a selective inhibitor of VEGF receptor-2 tyrosine kinase, and identification of its potential therapeutic window

Naoki Matsunaga,[1] Kazuhide Nakamura,[2] Atsushi Yamamoto,[2] Eri Taguchi,[2] Hiromi Tsunoda,[2] and Kazumi Takahashi[2]

[1]CMC R&D Laboratories and [2]Pharmaceutical Development Laboratories, Kirin Brewery Co. Ltd., Takasaki, Gunma, Japan

Abstract

KRN633 is a potent inhibitor of vascular endothelial growth factor (VEGF) receptor tyrosine kinases. However, it is poorly water-soluble; consequently, relatively high doses are required to achieve substantial *in vivo* tumor growth suppression after oral administration. We subjected KRN633 to the solid dispersion technique to improve its solubility, absorption, and antitumor efficacy after oral administration. This technique transformed the drug into an amorphous state and dramatically improved its dissolution rate. It also enhanced the bioavailability of the drug in rats by ~7.5-fold. The solid dispersion form of KRN633 also dramatically inhibited human tumor growth in murine and rat xenograft models: similar rates of tumor growth inhibition were obtained with 10- to 25-fold lower doses of the solid dispersion preparation relative to the pure drug in its crystalline state. Histologic analysis of tumors treated with the solid dispersion preparation revealed a significant reduction in microvessel density at much lower doses when compared with the crystalline form preparation. In addition, a dose-finding study using the solid dispersion form in a rat xenograft model revealed that there was a substantial range of doses at which KRN633 in the solid dispersion form showed significant antitumor activity but did not induce weight loss or elevate total urinary protein levels. These data suggest that the solid dispersion technique is an effective approach for developing KRN633 drug products and that KRN633 in the solid dispersion form may be a highly potent, orally available drug with a wide therapeutic window for diseases associated with abnormal angiogenesis. [Mol Cancer Ther 2006;5(1):80–8]

Introduction

Angiogenesis is deeply involved in tumor malignancy processes, such as tumor growth or metastasis (1). Several studies have analyzed the molecular regulation of angiogenesis and have found that vascular endothelial growth factor (VEGF) plays a central role in tumor angiogenesis. VEGF regulates both vascular proliferation and permeability and functions as an antiapoptotic factor for newly formed vessels. It binds to two high-affinity receptor tyrosine kinases on endothelial cells [i.e., VEGF receptor (VEGFR)-1 and VEGFR-2]. VEGFR-2 is the more functionally important stimulator of angiogenesis and vascular permeability (reviewed in refs. 2–4). The central role of VEGF and its receptor kinases in tumor angiogenesis makes targeting these molecules a promising approach in the development of antiangiogenic therapy. To this end, VEGF-neutralizing antibodies and small-molecule inhibitors of the VEGFR tyrosine kinases are currently being developed (4, 5). In particular, bevacizumab, a recombinant humanized monoclonal antibody specific for VEGF, has been approved as a first-line therapy for metastatic colorectal cancer because it significantly prolongs the overall and progression-free survival of patients in combination with 5-fluorouracil-based chemotherapy (6). The proof-of-concept accomplished by bevacizumab has promoted the development of orally bioavailable small molecules that target the VEGFR tyrosine kinases, several of which are now under preclinical or clinical development (7–13).

We reported previously a novel quinazoline urea derivative that targets the VEGFR tyrosine kinases and is denoted as KRN633 (14). KRN633 selectively inhibits the enzymatic activities of VEGFR-1, VEGFR-2, and VEGFR-3 tyrosine kinases *in vitro*. Consequently, KRN633 suppresses VEGF-induced VEGFR-2 phosphorylation in endothelial cells with an IC_{50} of 1.16 nmol/L; it also blocks the activation of mitogen-activated protein kinases and the proliferation of endothelial cells with IC_{50}s of 3.5 to 15 nmol/L. Moreover, KRN633 is well tolerated and suppresses tumor angiogenesis and growth in animals after being orally given daily. However, despite the potent *in vitro* antiangiogenic activity of KRN633, relatively high

Received 6/17/05; revised 10/6/05; accepted 10/24/05.

The costs of publication of this article were defrayed in part by the payment of page charges. This article must therefore be hereby marked advertisement in accordance with 18 U.S.C. Section 1734 solely to indicate this fact.

Note: N. Matsunaga, K. Nakamura, and A. Yamamoto contributed equally to this work.

Requests for reprints: Kazuhide Nakamura, Pharmaceutical Development Laboratories, Kirin Brewery Co. Ltd., 3 Miyahara, Takasaki, Gunma 370-1295, Japan. Phone: 81-27-346-9423; Fax: 81-27-347-5280. E-mail: ka-nakamura@kirin.co.jp

Copyright © 2006 American Association for Cancer Research.

doi:10.1158/1535-7163.MCT-05-0202

Downloaded from mct.aacrjournals.org on November 29, 2021. © 2006 American Association for Cancer Research.

doses were required to achieve substantial *in vivo* suppression. It may be that the low water solubility of KRN633 interferes with its absorption, which leads to its relatively poor performance *in vivo* with regard to its efficacy and toxicity.

The solid dispersion technique is one way to increase the dissolution rate and oral bioavailability of poorly water-soluble drugs. This technique involves complexing the drug in question with various excipients. This transforms the drug into a completely or partially amorphous form and thereby modifies its solubility. Several previous reports have documented the use of solid dispersion to enhance the solubility, dissolution rate, and oral bioavailability of poorly water-soluble compounds (15–20).

In this report, we describe the solid dispersion of KRN633 and show that it improves the solubility of the drug along with its absorption and antitumor efficacy after oral administration. In addition, we used the solid dispersion form of KRN633 to directly assess its therapeutic window.

Materials and Methods

Preparation of the Solid Dispersion and Physical Mixture Forms of KRN633

The crystal form of KRN633, which is identical to the preparation used in our previous study (14), was used throughout this study. The solid dispersion form of KRN633 mixed with the excipient polyvinylpyrrolidone (Wako Pure Chemical Industries, Ltd. Osaka, Japan) was obtained as follows. KRN633 (2 g crystal form) and polyvinylpyrrolidone (8 g) were mixed in 100 mL chloroform and then evaporated rapidly by using a rotary evaporator at 60°C followed by vacuum drying at 50°C. The physical mixture form composed of KRN633 and polyvinylpyrrolidone (KRN633/polyvinylpyrrolidone = 1/4) was prepared by simply mixing KRN633 with polyvinylpyrrolidone in a sample tube for 2 minutes.

Confirmation of the Physical Characteristics of the Solid Dispersion Form of KRN633

Powder X-ray diffraction analysis was done by using the Rigaku RINT 2200 Ultima X-ray diffraction apparatus with CuKá radiation at 40 kV and 40 mA at room temperature. The scanning rate was 5°C/min and the diffraction angle (2θ) was 3° to 40°. A Perkin-Elmer Pyris 1 differential scanning calorimeter was used to determine the differential scanning calorimeter thermal trace. The samples were encapsulated in ventilated aluminum pans and heated at a rate of 40°C/min over a temperature range of 30°C to 260°C. The surface topography was observed by using a Hitachi S-800 scanning electron microscope (SEM). The samples were fixed on a board using double-faced adhesive tape and the SEM was operated at an acceleration voltage of 20 kV.

Dissolution Test

A dissolution test was carried out according to the Japanese Pharmacopoeia XIV paddle method at an agitation speed of 100 rpm. Samples equivalent to 100 mg KRN633 were placed into a dissolution vessel with 900 mL Japanese Pharmacopoeia disintegration test fluid 1 (artificial gastric juices) and maintained at 37°C. Aliquots of the dissolution medium were collected every 3 minutes and filtered through a 10-μm filter. The UV wavelength for the detection was set at 290 nm.

Stability Test

The stability of the solid dispersion form of KRN633 was monitored over 7 months. The preparation was stored under three different conditions (room temperature, 40°C plus 75% relative humidity, and 73°C) for the indicated times. Its chemical stability was then evaluated by using high-performance liquid chromatography.

In vivo Absorption Study in Rats

Male Sprague-Dawley rats [Crl:CD(SD)] obtained from Charles River Japan, Inc. (Tokyo, Japan) were used in this study. KRN633 crystal form or solid dispersion preparations were given orally in a 0.5% methylcellulose suspension to rats at a dose of ~3.0 mg equivalent KRN633/kg. An additional group of rats received a single i.v. bolus dose of KRN633 in 5% dimethylacetamide/10% polyethylene glycol 400/30% ethanol aqueous solution at 0.1 mg equivalent KRN633/kg. Blood samples were collected from the tail vein at predetermined intervals for up to 72 hours after administration. The serum concentrations of KRN633 were determined as described previously (14). Briefly, serum samples were extracted with methyl-*t*-butyl ether and analyzed by high-performance liquid chromatography tandem mass spectrometry. Pharmacokinetic variables [area under the serum concentration-time curve extrapolated to infinity (AUC_∞) and apparent elimination half-life ($t_{1/2}$)] were calculated by noncompartmental analysis. The maximum serum concentration (C_{max}) and the time at which the C_{max} was achieved (T_{max}) were taken directly from the concentration data. The AUC_∞ and C_{max} were dose normalized to avoid variability in the dose concentration. The oral bioavailability was estimated by dividing the dose-normalized AUC_∞ (AUC_{norm}) resulting from oral administration by the AUC_{norm} resulting from i.v. administration. Statistical analysis of the AUC_{norm} was done using one-way AVOVA followed by Tukey's multiple comparison test. Analyses of the dose-normalized C_{max} ($C_{max,norm}$), T_{max}, and $t_{1/2}$ were carried out using one-way ANOVA followed by the Games-Howell's multiple comparison test.

Tumor Xenograft Models, Determination of Urinary Protein Levels, and Calculation of AUC_∞

The animal experiments were conducted as described previously (14). Briefly, the human prostate cancer cell lines PC3 and DU145 and the human lung tumor line A549 were cultured in appropriate medium and then implanted s.c. into the hind flanks of athymic mice (BALB/cA, Jcl-nu) or athymic rats (F344/N, Jcl-rnu). To facilitate the tumor grafting, PC3 or DU145 cells were suspended in Matrigel (BD Biosciences Discovery Labware, Bedford, MA) and diluted 1:1 in the relevant medium before implantation. The mice and rats were grouped randomly when the tumors reached the appropriate average volume (day 0).

Downloaded from mct.aacrjournals.org on November 29, 2021. © 2006 American Association for Cancer Research.

The animals then received the crystal form or solid dispersion preparations or vehicle (0.5% methylcellulose) once daily by oral gavage (as described in figure legends). The tumor volume was measured twice weekly. The percentage of tumor growth inhibition (TGI%), regression rate, and statistical significance were evaluated as described previously (14). On days 13 and 14, each individual rat was placed in a metabolic cage and its urine was collected over 24 hours. The urinary protein levels were measured by using commercial kits (Wako Pure Chemical Industries) and standard colorimetric methods. Additional athymic rats were also used to confirm *in vivo* exposure levels of KRN633 after a single oral administration of the crystal form or solid dispersion preparations at three different doses (as described in Table 2). Blood samples were collected at predetermined intervals, after which the serum concentrations of KRN633 were determined. The AUC_{∞} values were calculated as described above.

Histologic Analysis of A549 Tumors

A549 tumor xenografts were established in athymic mice as described above. The mice ($n = 5$) received the crystal form or solid dispersion preparations or vehicle once daily by oral gavage for 7 days (days 0–6). On day 7, tumor specimens were collected and fixed in 4% paraformaldehyde for 24 hours. The specimens were then paraffin-embedded and sectioned. Tumor microvessels were visualized by immunohistochemical detection using biotinylated anti-mouse CD31 antibody (BD PharMingen, San Diego, CA), horseradish peroxidase–labeled streptavidin (Invitrogen Corp., Carlsbad, CA), and a substrate kit (Vector Laboratories, Inc., Burlingame, CA). All of the sections were counterstained with hematoxylin. Three images of a viable region were captured for each section at ×200 magnification and the $CD31^+$ areas were subjected to computer-assisted image analysis by using Win ROOF software (Mitani Corp., Fukui, Japan).

Results

Physical Characterization of the Solid Dispersion Form of KRN633 and Analysis of Its Dissolution *In vitro*

Polyvinylpyrrolidone was selected as the carrier of the solid dispersion of KRN633 and simple evaporation was employed to generate the solid dispersion form of KRN633. To confirm the physical characteristics of KRN633 were changed by the solid dispersion, X-ray diffraction and differential scanning calorimeter analyses were done. In the X-ray diffraction study (Fig. 1A), the physical mixture preparation of KRN633 mixed with polyvinylpyrrolidone showed several peaks characteristic of the crystal form of KRN633. In contrast, the solid dispersion preparation of KRN633 showed a pattern that indicates KRN633 is in an amorphous form, as no distinctive peaks were observed. The endothermal peak of the crystal form at ~240°C in the differential scanning calorimeter thermogram was attributed to the melting of KRN633 (Fig. 1B). The physical mixture also showed a slight peak at ~240°C. However, no peak was observed for the solid dispersion preparation. These data indicate that the drug substance in the solid dispersion preparation was transformed into an amorphous state. SEM images of the physical mixture and solid dispersion preparations are shown in Fig. 1C. The drug substance appeared on the surface of the polyvinylpyrrolidone in the physical mixture, whereas the solid dispersion preparation showed completely uniform KRN633 and polyvinylpyrrolidone distribution.

A dissolution study was done using Japanese Pharmacopoeia disintegration test fluid 1 (artificial gastric juices) as the solvent (Fig. 1D). The dissolution rate of the crystal form was extremely low and did not even reach 10% during 2 hours. The early dissolution of the physical mixture was greater than that of the crystal form. However, it also did not reach 10%, which suggests that there is no substantial change in the physical state of the drug. In contrast, the dissolution of the solid dispersion was much better as it reached ~30% in 1 hour. These results indicate considerable differences in the dissolution rates of the crystal form and solid dispersion form of KRN633.

Table 1. Pharmacokinetic variables of KRN633 crystal form and KRN633 solid dispersion in male rats after being given orally once at 3 mg/kg

Variable	Solid dispersion, mean ± SD ($n = 3$)	Crystal form, mean ± SD ($n = 3$)
$C_{max,norm}$ (μg/mL/mg/kg)	2.29 ± 0.41*	0.269 ± 0.09
T_{max} (h)	3.33 ± 1.15	4.00 ± 0.00
AUC_{norm} (μg h/mL/mg/kg)	25.4 ± 2.10*	3.38 ± 1.30
$t_{1/2}$ (h)	7.93 ± 2.38	6.84 ± 2.02
Bioavailability (%)	65.8 ± 5.3*	8.8 ± 3.3

*$P < 0.05$ (versus crystal form).

Analyses of the Stability of the Solid Dispersion Form of KRN633

The chemical stability of the solid dispersion preparation of KRN633 was analyzed because the transformation of a molecule into an amorphous state sometimes leads to stability problems due to its high energy (21). When the solid dispersion preparation was stored at room temperature, its purity, as judged by high-performance liquid chromatography, decreased from an initial purity of 98.7% to a purity of 96.5% (2.2%) after 7 months. In contrast, when stored at 73°C for the same length of time, considerable degradation (6.7%) was observed. When stored at 40°C plus 75% relative humidity for 7 months, the purity decreased only by 2.8%; however, the solid dispersion preparation appeared as an agglutinated powder (data not shown). This is attributed to the high hygroscopicity of polyvinylpyrrolidone. In addition, physical stability studies, such as SEM or X-ray diffraction, did not detect major changes in the amorphous state of the solid dispersion preparation when it was stored at room temperature for at least 3 months (data not shown). Thus, the solid dispersion preparation of KRN633 seems to be quite stable when stored under dry and low temperature conditions.

Downloaded from mct.aacrjournals.org on November 29, 2021. © 2006 American Association for Cancer Research.

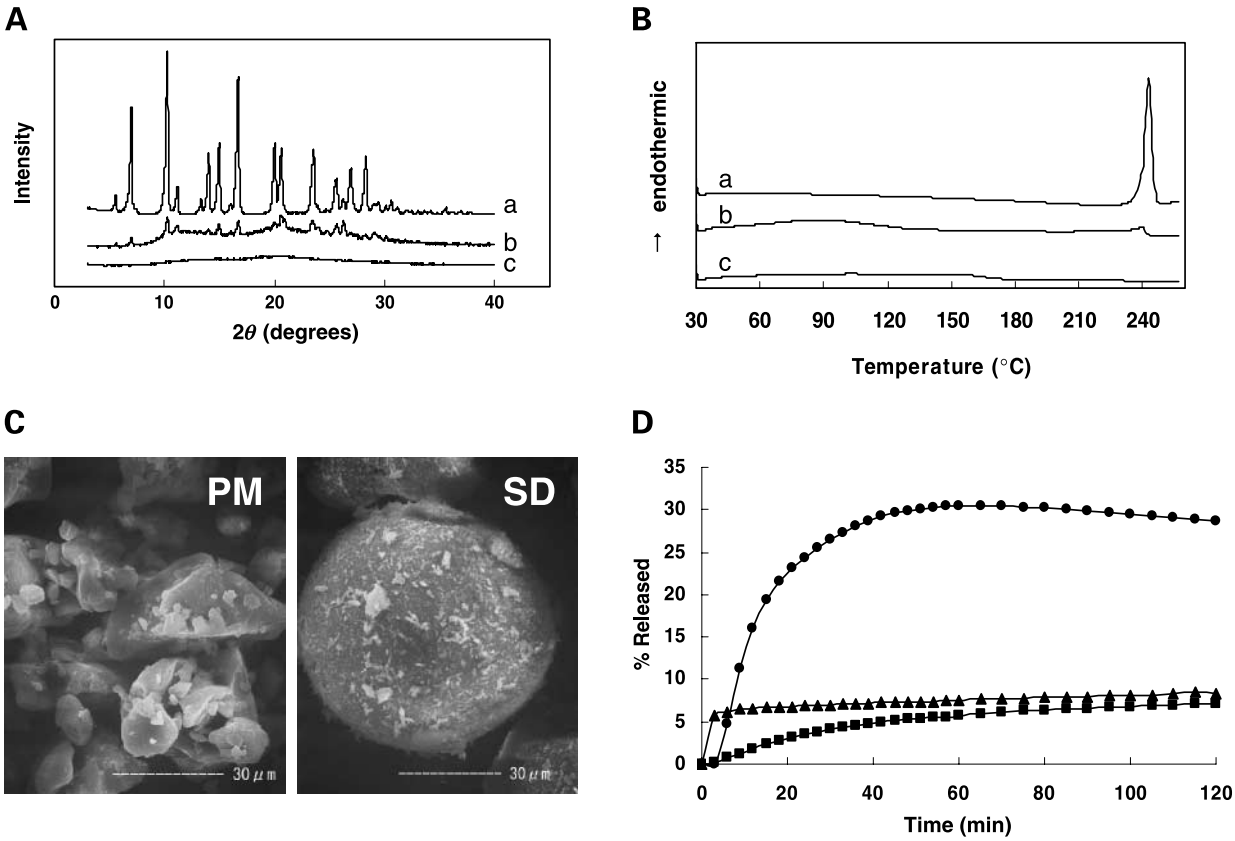

Figure 1. Physical characteristics and dissolution profile of KRN633 solid dispersion. **A,** X-ray diffraction patterns of the crystal form (*a*), physical mixture (*b*), and solid dispersion (*c*) preparations of KRN633. The solid dispersion preparation showed a typical halo pattern of the amorphous form without distinctive peaks. **B,** representative differential scanning calorimeter thermograms of the crystal form (*a*), physical mixture (*b*), and solid dispersion (*c*) preparations of KRN633. The amorphous form of KRN633 in the solid dispersion preparation is indicated by the disappearance of the endothermal peak at ~240°C. **C,** SEM analyses of the physical mixture (*PM; left*) and solid dispersion (*SD; right*) preparations of KRN633. **D,** dissolution profiles of KRN633 in its crystal form (■), physical mixture (▲), and solid dispersion (●) forms.

Pharmacokinetics of the Solid Dispersion Preparation of KRN633 in Rats after Its Oral Administration

Rats were given the crystal form and solid dispersion preparations of KRN633 once orally and the concentrations of KRN633 in their sera were measured. Significantly higher serum concentrations were observed when the solid dispersion preparation was given, indicating its enhanced drug absorption compared with that of the crystal form preparation (Fig. 2). The $C_{max,norm}$ and bioavailability of the solid dispersion preparation were ~8.5 and 7.5 times greater than those of the crystal form preparation, respectively (Table 1). In contrast, the T_{max} and $t_{1/2}$ values were equivalent for the solid dispersion and crystal form preparations.

Solid Dispersion Preparation Is More Potent against Human Tumor Xenografts in Mice Than the Crystal Form Preparation

The antitumor activities of the crystal form and solid dispersion preparations were evaluated in athymic mice bearing human tumor xenografts. In the A549 human lung tumor xenograft model (Fig. 3A), once daily oral administration of the crystal form preparation inhibited tumor growth in a dose-dependent manner during the 2-week treatment: the TGI% at day 12 was 65.2 and 89.8 for 20 and 100 mg/kg, respectively. In contrast, the solid dispersion preparation inhibited tumor growth more dramatically and at lower doses than the crystal form preparation. Consequently, the TGI% at day 12 of the 4 mg/kg solid dispersion preparation was comparable with that of 100 mg/kg crystal form (90.2 versus 89.8). Moreover, administering 20 and 100 mg/kg solid dispersion led to 31.4% and 45.0% tumor regression, respectively. In addition, sustained TGI was observed after the treatment with 100 mg/kg solid dispersion ceased.

We confirmed the profound antitumor activities of the solid dispersion preparation by using the DU145 and PC3 human prostate tumor xenograft models (Fig. 3B and C). This revealed that although all doses of KRN633 led to tumor regression in the DU145 xenograft model the regression rates at day 14 induced by 4 and 20 mg/kg solid dispersion (26.3% and 58.1%, respectively) were greater than that induced by 100 mg/kg crystal form (6.7%). With regard to the PC3 xenograft model,

Downloaded from mct.aacrjournals.org on November 29, 2021. © 2006 American Association for Cancer Research.

the TGI% at day 14 induced by the 4 mg/kg solid dispersion preparation was comparable with that induced by 100 mg/kg crystal form (35.3 versus 31.4), and this was exceeded by the 20 mg/kg solid dispersion dose.

Effect of the Solid Dispersion Preparation on *In vivo* Tumor Growth, Body Weight, and Total Urinary Protein in Tumor-Bearing Athymic Rats

The enhanced antitumor activity of the solid dispersion preparation was confirmed in athymic rats bearing A549 tumor xenografts (Table 2). Tumor growth was almost completely suppressed by administering the solid dispersion preparation at a dose of 1 mg/kg during the treatment period (TGI% at day 14 was 82.1). Moreover, the tumors regressed when treated with the solid dispersion preparation at a dose of ≥3 mg/kg. In contrast, the crystal form preparation was significantly less potent in its antitumor activity, as it showed no significant activity at a dose of 1 mg/kg, produced only a moderate TGI at 10 mg/kg (TGI% at day 12 = 75.2), and only induced near-complete TGI at a dose of 100 mg/kg, which induced slight regression (regression rate = 3.7%). Thus, doses of 1 mg/kg solid dispersion and 10 to 50 mg/kg crystal form resulted in similar TGI (~80%) in rats. This suggests that the solid dispersion preparation has at least 10-fold greater antitumor activity compared with the crystal form preparation. In line with this was that the AUC_{∞} after administering the crystal form preparation at 100 mg/kg was markedly lower than that of the solid dispersion preparation at 10 mg/kg (9.4 versus 33.7 μg h/mL).

The rats that received 30 and 100 mg/kg of the solid dispersion preparation exhibited severe weight loss (i.e., a 10.7% reduction on day 14 and a 20.8% reduction on day 18 relative to their initial weight, respectively). Moreover, one rat that received 100 mg/kg of the solid dispersion preparation died on day 21 (data not shown). However,

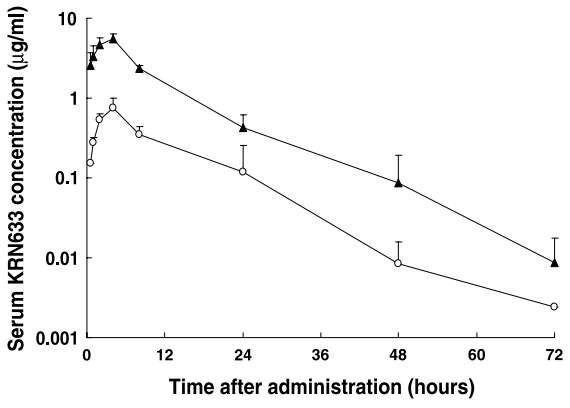

Figure 2. Mean serum concentrations of KRN633 after a single oral administration of a 3.0 mg/kg dose in Sprague-Dawley rats. KRN633 was given in the crystal form (○) or solid dispersion form (▲). Both compounds were suspended in vehicle (0.5% methylcellulose in distilled water). *Points,* mean (n = 3); *bars,* SD.

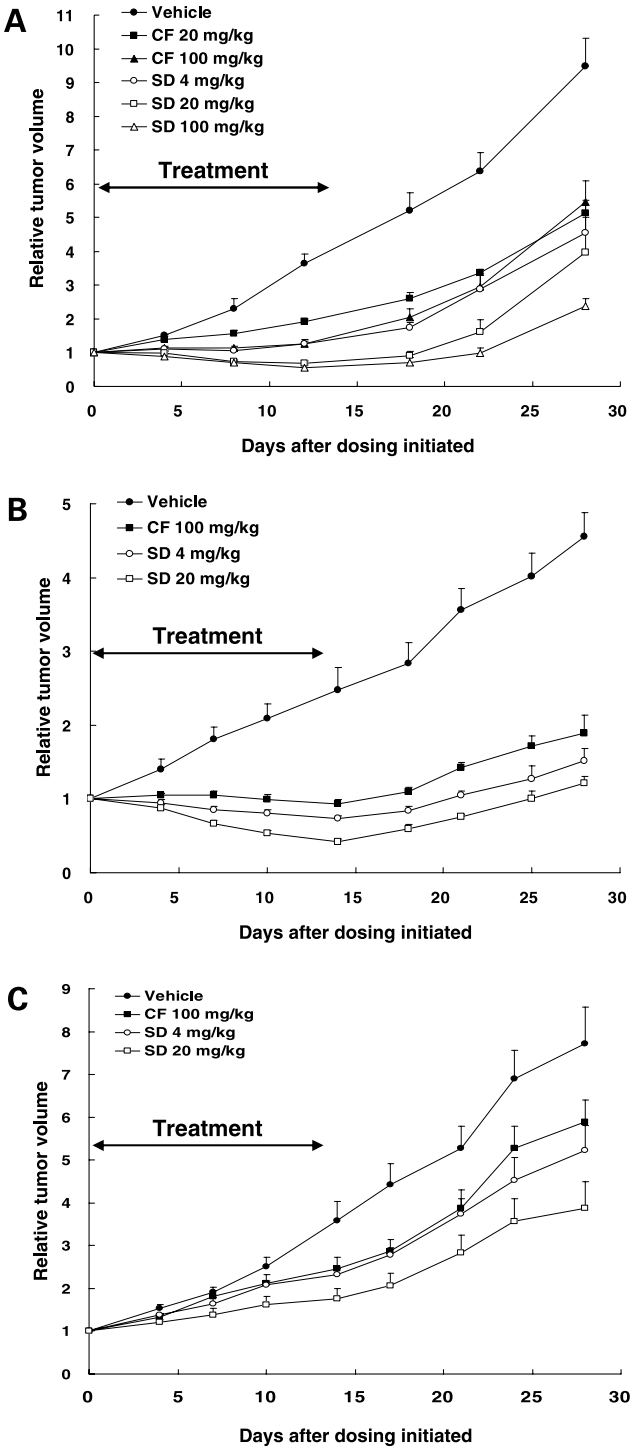

Figure 3. Effect of the crystal form and solid dispersion preparations of KRN633 on the growth of human tumor xenografts in mice. A549 human lung carcinoma (**A**), DU145 human prostate carcinoma (**B**), or PC3 human prostate carcinoma (**C**) tumors were established after the s.c. implantation of tumor cells into the flanks of athymic mice. Tumor-bearing mice were randomized into several groups when the tumors reached an average size of 105 mm^3 (A549), 150 mm^3 (DU145), or 150 mm^3 (PC3). Daily oral administration of the crystal form or solid dispersion preparation was initiated on the day of randomization and continued for 2 wks (n = 5). *Points,* mean tumor volumes; *bars,* SE.

Downloaded from mct.aacrjournals.org on November 29, 2021. © 2006 American Association for Cancer Research.

Table 2. Comparison of the effects of the crystal form and solid dispersion preparations of KRN633 on A549 tumor-bearing athymic rats

Dose (mg/kg)	Solid dispersion treated					Crystal form treated		
	TGI%	Regression (%)	Weight loss (%)*	Total urinary protein (mg/dL)	AUC_∞ (μg h/mL)	TGI%	Regression (%)	AUC_∞ (μg h/mL)
Vehicle				2.9				
0.1	19.4	—	—	6.0				
0.3	21.9	—	—	5.2				
1	82.1 †	—	—	2.6	5.1	14	—	
2						9.6	—	
3	>100 †	19.3	—	4.5				
5						33.9	—	2.3
10	>100 †	34.8	—	13.8	33.7	75.2 ‡	—	
20						60.6	—	6.5
30	>100 †	45.6	10.7 (d 14)	57.9 †				
50						81.1§	—	
100	>100 †	42.8	20.8 (d 18)	ND‖	76.6	>100 †	3.7	9.4

NOTE: The effects of the crystal form and solid dispersion preparations were evaluated by separate experiments. A549 human lung carcinoma tumors were established after the s.c. implantation of tumor cells into the flank of athymic rats. After randomization, daily oral administration of the crystal form or solid dispersion preparations was initiated and continued for 2 weeks ($n = 5$). The average initial tumor volumes (day 0) of the rat groups used to evaluate the efficacy of the crystal form and solid dispersion preparations were 162 and 231 mm^3, respectively. The TGI% induced by the solid dispersion and crystal form preparations was determined at days 14 and 12, respectively. On days 13 and 14, each rat was placed in a metabolic cage and its urine was collected over 24 hours.

*Amount of maximum weight reduction from the initial weight at day 0 during the study (the corresponding day is indicated in brackets; losses that are >1% of the initial weight are shown). $AUC_\infty$was derived from the serum concentrations of KRN633 after a single oral administration at each dose in athymic rats.

†$P < 0.001$ (KRN633-treated groups versus vehicle-treated group).

‡$P < 0.01$.

§$P < 0.05$.

‖ND, not determined.

the body weights of the remaining rats recovered to control levels within 2 weeks after drug withdrawal. Notably, solid dispersion preparation doses of ≤10 mg/kg had no significant effect on the body weight or general behavior of the rats.

Total urinary protein was also assessed as a noninvasively measurable indicator of the toxicity in the same study. Administration of the solid dispersion preparation at 30 mg/kg for 14 days significantly increased total urinary protein levels. However, administration at ≤10 mg/kg had no effect on urinary protein levels.

When equivalent studies were done with athymic mice, none of the mice showed significant weight loss or had died by the end of the study (data not shown).

Solid Dispersion Preparation Potently Reduces Microvessel Density in Murine Tumors

Treatment of A549 tumor-bearing mice with the crystal form preparation at 100 mg/kg for 7 days reduced the microvessel density ($CD31^+$ endothelial cells) in viable tumor regions by 67.6% when compared with vehicle-treated controls (Fig. 4A, C, and F). In contrast, treatment with the solid dispersion preparation at 4 or 20 mg/kg for 7 days significantly reduced microvessel density by 51.7% or 80.7%, respectively (Fig. 4A and D–F). These reductions in tumor microvessel density correlated closely with the degree of TGI achieved by the various treatments (data not shown).

Discussion

Improving the dissolution characteristics of poorly water-soluble drug substances is important for achieving good oral bioavailability. It is common practice during drug development to introduce functional groups into drugs that enhance their water solubility. However, this sometimes alters the principal pharmacologic characteristics of the drugs. In the present study, we applied the solid dispersion technique to KRN633, which is poorly water-soluble but has well-characterized and potent *in vitro* activities. We found that this markedly improved the dissolution rate of KRN633 along with its oral bioavailability and pharmacologic efficacy without changing its principal pharmacologic characteristics.

The solid dispersion preparation of KRN633 was prepared by simply evaporating the chloroform solution containing polyvinylpyrrolidone (a pharmacologically inert polymeric material) and KRN633. X-ray diffraction analysis of this preparation showed no peaks characteristic of the crystal form preparation, and differential scanning calorimeter analysis revealed no endothermal peaks. In addition, the SEM image of the solid dispersion preparation showed complete uniformity of KRN633 and polyvinylpyrrolidone distribution. These data suggest that the drug in the solid dispersion preparation is mainly in an amorphous state. More importantly, the transformation of KRN633 into the amorphous state successfully increased its

Downloaded from mct.aacrjournals.org on November 29, 2021. © 2006 American Association for Cancer Research.

dissolution rate in Japanese Pharmacopoeia disintegration test fluid 1. Because amorphous states sometimes lead to stability problems because of their high energy (21), we also analyzed the stability of KRN633 in the solid dispersion preparation. When this preparation was stored under conditions of high humidity and temperature, considerable physical and chemical changes were observed. However, under normal storage conditions, the solid dispersion preparation was stable enough to be suitable for clinical applications.

Along with its increased solubility, the oral bioavailability of KRN633 in rats was significantly increased (by ~7.5-fold) when it was in the solid dispersion form compared with when it was in the crystal form. Because the crystal form and solid dispersion form did not differ significantly in T_{max} and $t_{1/2}$, the enhanced oral bioavailability of the solid dispersion form is probably due to its improved absorption. Moreover, the antitumor activities of KRN633 were dramatically enhanced by its formulation as a solid dispersion form. The solid dispersion form inhibited the growth of human tumor xenografts at much lower doses than the crystal form preparation in both mice and rats. It seems that the solid dispersion preparation acts comparably *in vivo* with the crystal form preparation at least 10-fold lower doses in rats and at ~25-fold lower doses in mice. Similarly, the solid dispersion form reduced the microvessel density in the murine tumors at considerably lower doses than the crystal form preparation. Notably, this indicates not only that the solid dispersion form is a more effective antitumor agent than the crystal form at equivalent doses but also that its *in vivo* mechanism of action is like that of the crystal form preparation (i.e., the inhibition of tumor angiogenesis by primarily targeting the tumoral endothelial cells). We reported previously that the antitumor activities of KRN633 are likely to depend on the length of time that the serum concentration remains above the target concentration (14). The enhanced oral bioavailability of the solid dispersion preparation would extend the period of this target suppression (suppression of angiogenesis) at lower doses. Incidentally, it should be noted that although solid dispersion showed enhanced antitumor activities with all the tumors that we tested the PC3 tumor seemed to be less susceptible to KRN633. The factors that affect susceptibility to KRN633 remain to be clarified by follow-up studies.

We reported previously that KRN633 was well tolerated and had no significant effects on the body weight and general behavior of mice and rats (14). However, the low absorbance of KRN633 in the crystal form preparation

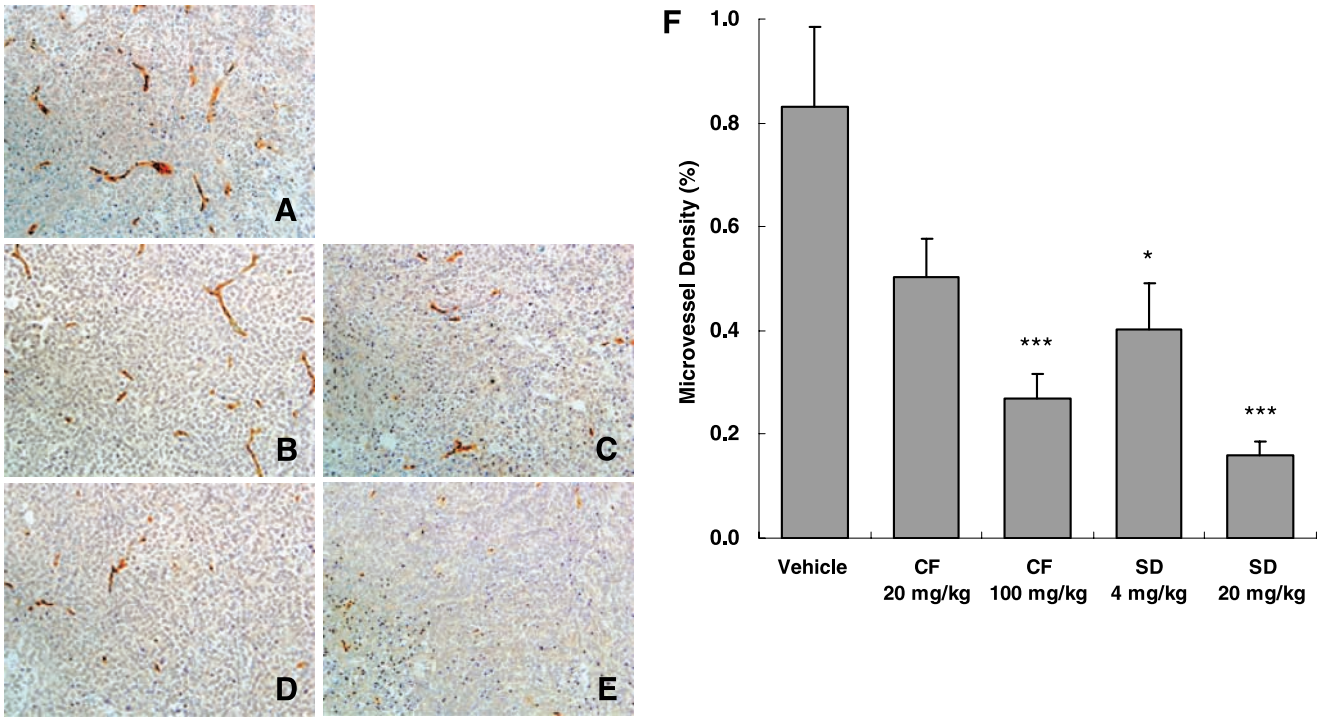

Figure 4. Effect of the crystal form and solid dispersion preparations of KRN633 on tumor microvessel density. Athymic mice bearing A549 tumors were treated once daily for 7 d with the crystal form or solid dispersion preparations of KRN633 at the doses indicated or with vehicle. The tumors were then harvested from the mice treated with vehicle (**A**), the crystal form preparation at 20 (**B**) or 100 (**C**) mg/kg, or the solid dispersion preparation at 4 (**D**) or 20 (**E**) mg/kg. Paraformaldehyde-fixed, paraffin-embedded tumor sections were prepared and the $CD31^+$ cells were immunohistochemically stained to visualize the blood vessels. **F,** microvessel density (percentage of $CD31^+$ area per tumor area) was determined by image analysis. *Columns,* mean; *bars,* SE. *, $P < 0.05$; ***, $P < 0.001$, treated groups versus control (vehicle) group (Dunnett's test).

Downloaded from mct.aacrjournals.org on November 29, 2021. © 2006 American Association for Cancer Research.

in this previous study may have limited the *in vivo* toxicity of the drug along with its efficacy. The AUC_∞ after administration of the crystal form preparation was not linear with respect to doses at 5, 20, and 100 mg/kg in athymic rats (it was 2.3, 6.5, and 9.4 μg h/mL, respectively), and the AUC_∞ of the crystal form preparation at 100 mg/kg was less than that of the solid dispersion preparation at 10 mg/kg (9.4 versus 33.7 μg h/mL). At these doses, no signs of toxicity (weight loss or total urinary protein) were observed. These data suggest that it is not possible to induce toxicity with the crystal form preparation of KRN633 due to the exposure saturation at higher doses in this model.

Along with weight loss and behavior, total urinary protein was employed as a noninvasive indicator of the toxicity of KRN633, because it has been reported that adverse events in phase I and II studies of bevacizumab include proteinuria (22). Our results show that rats receiving ≥30 mg/kg of the solid dispersion preparation indeed exhibited elevated total urinary protein levels as well as weight loss. This effect of the 30 mg/kg solid dispersion preparation on urinary protein levels is probably because VEGF is important in the development and repair of renal glomerular capillaries (23–25). This is indicated by a study that showed the neutralization of VEGF with an antibody interrupted postnatal glomerular capillary development (23). Moreover, an antagonist of VEGF inhibited glomerular capillary repair in a recovery model of Thy-1 glomerulonephritis (24). In addition, the *in vivo* administration of VEGF enhanced capillary repair in severe glomerulonephritis (23, 24). Therefore, the kidney is sensitive to the blockade of VEGF signaling, which suggests that urinary protein may be a common toxicologic biomarker for long-term treatment with angiogenesis inhibitors that target the VEGF/VEGFR system.

Notably, although the 30 mg/kg solid dispersion preparation elevated total urinary protein levels, this did not occur in rats that received 10 mg/kg of the solid dispersion preparation. These data indicate that the maximum well-tolerated dose of the solid dispersion preparation in this model is at least 10 mg/kg. Given that the solid dispersion preparation significantly inhibits tumor growth at 1 mg/kg in the same model, it is conceivable that the therapeutic window of KRN633 with regard to its efficacious dosage is quite wide. However, how renal and tumor vasculatures differ in terms of their dependency on VEGF and sensitivity to VEGFR inhibitors should be determined before the safe and efficacious dose range can be established.

In summary, the solid dispersion form of KRN633 prepared with polyvinylpyrrolidone was superior to the corresponding crystal form preparation of KRN633 in terms of its rate of dissolution, oral bioavailability, and pharmacologic efficacy. Moreover, it showed a wide therapeutic window in terms of efficacious dosages. Thus, our study indicates that the solid dispersion of KRN633 not only improves the efficacy of this poorly water-soluble drug substance, KRN633, in the solid dispersion formulation but may also be a possible therapeutic agent for diseases associated with abnormal angiogenesis.

Acknowledgments

We thank Dr. Toru Miura, Dr. Masaru Kamishohara, and Masafumi Teshigawara for helpful discussions.

References

1. Bergers G, Benjamin LE. Tumorigenesis and the angiogenic switch. Nat Rev Cancer 2003;3:401–10.

2. Veikkola T, Karkkainen M, Claesson-Welsh L, Alitalo K. Regulation of angiogenesis via vascular endothelial growth factor receptors. Cancer Res 2000;60:203–12.

3. Ferrara N, Gerber HP, LeCouter J. The biology of VEGF and its receptors. Nat Med 2003;9:669–76.

4. Hicklin DJ, Ellis LM. Role of the vascular endothelial growth factor pathway in tumor growth and angiogenesis. J Clin Oncol 2005; 23:1011–27.

5. Ferrara N, Hillan KJ, Gerber HP, Novotny W. Discovery and development of bevacizumab, an anti-VEGF antibody for treating cancer. Nat Rev Drug Discov 2004;3:391–400.

6. Hurwitz H, Fehrenbacher L, Novotny W, et al. Bevacizumab plus irinotecan, fluorouracil, and leucovorin for metastatic colorectal cancer. N Engl J Med 2004;350:2335–42.

7. Wood JM, Bold G, Buchdunger E, et al. PTK787/ZK 222584, a novel and potent inhibitor of vascular endothelial growth factor receptor tyrosine kinases, impairs vascular endothelial growth factor-induced responses and tumor growth after oral administration. Cancer Res 2000;60:2178–89.

8. Mendel DB, Laird AD, Xin X, et al. *In vivo* antitumor activity of SU11248, a novel tyrosine kinase inhibitor targeting vascular endothelial growth factor and platelet-derived growth factor receptors: determination of a pharmacokinetic/pharmacodynamic relationship. Clin Cancer Res 2003;9:327–37.

9. Ruggeri B, Singh J, Gingrich D, et al. CEP-7055: a novel, orally active pan inhibitor of vascular endothelial growth factor receptor tyrosine kinases with potent antiangiogenic activity and antitumor efficacy in preclinical models. Cancer Res 2003;63:5978–91.

10. Beebe JS, Jani JP, Knauth E, et al. Pharmacological characterization of CP-547,632, a novel vascular endothelial growth factor receptor-2 tyrosine kinase inhibitor for cancer therapy. Cancer Res 2003;63: 7301–9.

11. Wilhelm SM, Carter C, Tang L, et al. BAY 43-9006 exhibits broad spectrum oral antitumor activity and targets the RAF/MEK/ERK pathway and receptor tyrosine kinases involved in tumor progression and angiogenesis. Cancer Res 2004;64:7099–109.

12. Sepp-Lorenzino L, Rands E, Mao X, et al. A novel orally bioavailable inhibitor of kinase insert domain-containing receptor induces antiangiogenic effects and prevents tumor growth *in vivo*. Cancer Res 2004;64: 751–6.

13. Wedge SR, Kendrew J, Hennequin LF, et al. AZD2171: a highly potent, orally bioavailable, vascular endothelial growth factor receptor-2 tyrosine kinase inhibitor for the treatment of cancer. Cancer Res 2005;65: 4389–400.

14. Nakamura K, Yamamoto A, Kamishohara M, et al. KRN633: a selective inhibitor of vascular endothelial growth factor receptor-2 tyrosine kinase that suppresses tumor angiogenesis and growth. Mol Cancer Ther 2004;3:1639–49.

15. Goldberg AH, Gibaldi M, Kanig JL. Increasing dissolution rates and gastrointestinal absorption of drugs via solid solutions and eutectic mixtures. I. Theoretical considerations and discussion of the literature. J Pharm Sci 1965;54:1145–8.

16. Chiou WL, Riegelman S. Pharmaceutical applications of solid dispersion systems. J Pharm Sci 1971;60:1281–302.

17. Serajuddin AT. Solid dispersion of poorly water-soluble drugs: early promises, subsequent problems, and recent breakthroughs. J Pharm Sci 1999;88:1058–66.

Downloaded from mct.aacrjournals.org on November 29, 2021. © 2006 American Association for Cancer Research.

18. Shah N, Pytelewski R, Eisen H, Jarowski CI. Influence of dispersion method on dissolution rate and bioavailability of digoxin from triturations and compressed tablets II. J Pharm Sci 1974;63:339 – 44.

19. Kushida I, Ichikawa M, Asakawa N. Improvement of dissolution and oral absorption of ER-34122, a poorly water-soluble dual 5-lipoxygenase/cyclooxygenase inhibitor with anti-inflammatory activity by preparing solid dispersion. J Pharm Sci 2002;91:258 – 66.

20. Yamashita K, Nakate T, Okimoto K, et al. Establishment of new preparation method for solid dispersion formulation of tacrolimus. Int J Pharm 2003;267:79 – 91.

21. Ambike AA, Mahadik KR, Paradkar A. Stability study of amorphous valdecoxib. Int J Pharm 2004;282:151 – 62.

22. Sandler AB, Johnson DH, Herbst RS. Anti-vascular endothelial growth factor monoclonals in non-small cell lung cancer. Clin Cancer Res 2004;10:4258 – 62s.

23. Kitamoto Y, Tokunaga H, Tomita K. Vascular endothelial growth factor is an essential molecule for mouse kidney development: glomerulogenesis and nephrogenesis. J Clin Invest 1997;99:2351 – 7.

24. Ostendorf T, Kunter U, Eitner F, et al. VEGF(165) mediates glomerular endothelial repair. J Clin Invest 1999;104:913 – 23.

25. Masuda Y, Shimizu A, Mori T, et al. Vascular endothelial growth factor enhances glomerular capillary repair and accelerates resolution of experimentally induced glomerulonephritis. Am J Pathol 2001;159:599 – 608.

Downloaded from mct.aacrjournals.org on November 29, 2021. © 2006 American Association for Cancer Research.

AACR American Association for Cancer Research

Molecular Cancer Therapeutics

Improvement by solid dispersion of the bioavailability of KRN633, a selective inhibitor of VEGF receptor-2 tyrosine kinase, and identification of its potential therapeutic window

Naoki Matsunaga, Kazuhide Nakamura, Atsushi Yamamoto, et al.

Mol Cancer Ther 2006;5:80-88.

Updated version Access the most recent version of this article at:
http://mct.aacrjournals.org/content/5/1/80

Cited articles This article cites 24 articles, 10 of which you can access for free at:
http://mct.aacrjournals.org/content/5/1/80.full#ref-list-1

Citing articles This article has been cited by 1 HighWire-hosted articles. Access the articles at:
http://mct.aacrjournals.org/content/5/1/80.full#related-urls

E-mail alerts Sign up to receive free email-alerts related to this article or journal.

Reprints and Subscriptions To order reprints of this article or to subscribe to the journal, contact the AACR Publications Department at pubs@aacr.org.

Permissions To request permission to re-use all or part of this article, use this link
http://mct.aacrjournals.org/content/5/1/80.
Click on "Request Permissions" which will take you to the Copyright Clearance Center's (CCC)
Rightslink site.

Downloaded from mct.aacrjournals.org on November 29, 2021. © 2006 American Association for Cancer Research.